Journal Name

COMMUNICATION

Desorption of CO from individual ruthenium porphyrin molecules on a copper surface by inelastic tunneling process

Received 00th January 20xx,
Accepted 00th January 20xx

DOI: 10.1039/x0xx00000x

www.rsc.org/

Takuma Omiya[ab], Paolo Poli[b], Heike Arnolds[b], RasmitaRaval[b], Mats Persson[b], and Yousoo Kim*[a]

The coordination of CO to metalloporphyrins changes their electronic and magnetic properties. Here we locally desorb CO molecules from a single ruthenium tetraphenylporphyrin carbonyl(CO-RuTPP)on Cu(110) with STM. The desorption is triggered by the injection of holes into the occupied states of the adsorbate with an unusual two-carrier process.

The formation and breaking of metal-carbonyl bonds has generated much interest because of their correlation with biological and catalytic properties such as the prevention of hemoglobin oxygen transport in living system[1] and CO poisoning in heterogeneous catalysis[2]. In addition, thermal and photo-induced metal-carbonyl bond breaking provides information about the bond strength and energy transfer[3]. The formation and breakage of a metal-carbonyl bond also makes it possible to control the electronic structure and physical properties of organometallic compounds. In particular, introducing carbon monoxide (CO) onto a metal atom at the centre of a metalloporphyrin provides additional versatility to its magnetic, electronic and optical properties for future applications in chemical sensing and molecular electronics[4]. For example, the coordination of CO onto RuTPP increases its electronic excitation lifetime 1000foldby switching the lowest excited state from a single (d,π*) to a triplet $^3(\pi,\pi^*)$state, leading to phosphorescence[5].

A scanning tunnelling microscope(STM) is a versatile tool for investigating chemical reactions and motions of a single molecule either by imaging or manipulating individual molecules. An important factor in driving chemical reactions when using the STM tip is the adsorbate-induced-resonance states, which can be identified in scanning tunnelling spectroscopy (STS). Tunnelling electrons are temporarily trapped in such a resonance state and create an electronically or vibrationally excited adsorbate, followed by the induction of motion or reaction before the energy is dissipated from the adsorbate into the metal substrate. For example, it has been shown that both desorption and diffusion of a CO molecule on Cu(111) were initiated at a threshold sample bias voltage V_s=2.4V, caused by a single electronic transition through electron injection into the CO 2π* state[6]. In contrast to CO on metal surfaces, very little work has focussed on desorption of CO from organometallic complexes adsorbed on metal surfaces, where the molecular complex electronically decouples CO from the metal substrate. The much weaker interaction between the CO and metal substrate and concomitant increase in lifetimes of electronically excited states should open up new reaction paths, since excited electrons need to be localized at the target chemical bond for a sufficiently long period to induce motion[7]. Only a few comparable studies have been made using tunnelling electron injection to the organometallic molecule from the tip of an STM[4A, 4B, 8]. Stróżecka *et al.* reported electric-field effect induced CO desorption from manganese phthalocyanine on Bi(110)[4B]. The authors observed a sudden drop in the tunnelling current (I_t) in the V_s range of 400–600 mV, which shows the threshold V_s increases linearly with the tip-sample distance. Meanwhile, energy transfer from the tunnelling electrons to the Co-NO bond through the IET process was inferred to induce the desorption of NO from NO-CoTPP/Au(111)[8B]. Interestingly, desorption of NO was observed as a two-carrier process at 0.8 V while it alters to a one-carrier process at 1.0 V. The proposed mechanism is vibrational ladder climbing of the Co-NO bond, where 1.0 V electrons are sufficient to lead to direct desorption, while two lower energy electrons need to arrive within the vibrational relaxation time to cause desorption[8B].

In this communication, we present a single-molecule investigation of the desorption of CO from the CO-RuTPP on a Cu(110) surface using a combination of scanning tunnelling spectroscopy (STS), reaction yield measurements and density functional theory calculations. The single-molecule study revealed that CO desorption is driven by IET with a two-carrier process.

All experiments were performed using a low-temperature STM (Scienta Omicron Inc\) at 4.7 K. A Cu(110) single crystal surface was cleaned using Ar^+ ion sputtering and annealing at 800 K. CO-RuTPP was purchased from Sigma Aldrich and transferred into the home made doser which was degassed over 12 h at ~150 °C in vacuum to remove solvents. The sublimation of CO-RuTPP onto a clean Cu(110) surface was performed by resistive heating to ~200 °C whilst holding

[a] *Surface and Interface Science Laboratory, RIKEN, Wako 351-0198, Japan E-mail: ykim@riken.jp; Fax: +81 48 467 1945; Tel: +81 48 467 4073*
[b] *Surface Science Research Centre and Department of Chemistry, University of Liverpool, Oxford Road, Liverpool L69 3BX, United Kingdom*

the substrate at room temperature. From the STM images, RuTPP on Cu(110) does not contain CO in this condition,

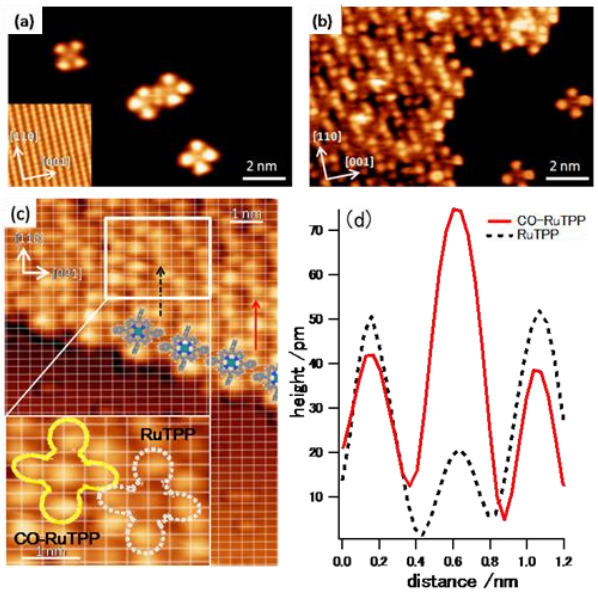

Fig 1 (a)–(c) STM images of (a)-(b) RuTPP and (c) CO-RuTPP adsorbed on Cu(110). The images were obtained at 4.7K with V_s = 500 mV and I_t = 0.5 nA. (a)(b) Inset: atomic resolution STM image of bare Cu(110)used to calibrate the distance and angle. (b) shows higher molecular coverage area than (a). (c)STM image of RuTPP coadsorbed with CO, which is superimposed on the Cu(110) lattice lines calibrated by CO/Cu(110). A ball and stick model of RuTPP is overlaid on the STM image. Inset enlarged image of RuTPP and CO-RuTPP, which are marked by dotted and solid lines, respectively. (d) Cross-sectional height profiles measured along the straight lines of RuTPP and CO-RuTPP on Cu(110). The corresponding solid and dotted lines are shown in (c).

due to CO-RuTPP decomposes into CO and RuTPP during the deposition process. To observe CO-RuTPP on the surface, CO molecules were therefore co-dosed onto the Cu(110) surface at ~50 K. The acquired images were processed using the WSxM[9] software to adjust image contrast and calibrate the distance.

Each RuTPP on Cu(110) displays bright protrusions, as shown in the STM images of Figs 1a–b. The STM images show a four-lobe structure in both cases of isolated molecules and those within molecular assemblies as shown in Fig 1a. Previous studies have also reported similar features in STM images, and assigned them to TPP molecules[10]. The angle and size of the STM images were calibrated using an atomically-resolved STM image of a bare Cu(110) surface, as shown in the inset of Fig. 1a.With increasing molecular coverage, the RuTPP molecule forms a regular and ordered array structure as shown in Fig. 1b. The STM images obtained from the DFT calculations (Fig. S2 in SI) reproduce well the observed STM images. Furthermore, they show that the four lobed protrusions are due to the distorted phenyl groups and that the protrusion in the centre of the molecule arises from CO adsorption. The adsorption site can be determined using a marker molecule with a known adsorption site. Here we used coadsorbed CO on bare Cu(110), as shown in Fig. 1c, which occupies atop sites[11]. The derived grid lines of the Cu(110) lattice are superimposed on the STM image and show that the ruthenium atom occupies a short bridge site. The four-lobe structure is aligned with the copper rows, which is consistent with the previous results for other metalloporphyrins on Cu(110)[10A, 12]. The short bridge site is stabilised by substrate-porphine hybridization, which leads to a short carbon-copper distance of 2.50 Å for CoTPP on Cu(110)[10A]. After CO exposure at ~50 K, the image

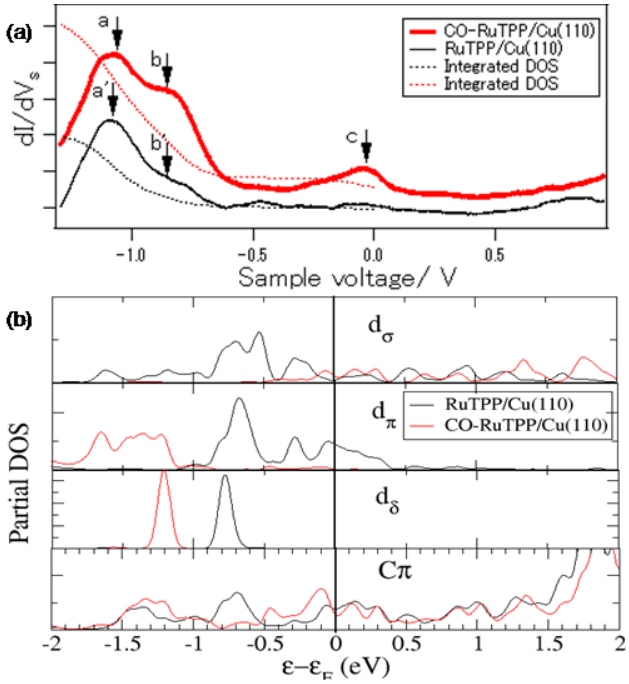

Fig. 2 a) STS spectra and b) calculated partial density of states (DOS) of CO-RuTPP(red lines) and RuTPP(black lines) on Cu(110) surface. a) The STS spectrum of bare Cu(110) is subtracted to emphasis the change in dI/dV_s. Dotted lines show the integrated STS signal from the Fermi level. Major peaks are labelled a-c for a guide of eyes. Assignment of peak a-d is discussed in text. b) The partial DOS is obtained for the indicated partial waves around the Ru and C.

contrast at the centre of RuTPP molecules becomes much brighter, indicating an attachment of CO on top of a ruthenium atom Fig.1(c),as also observed for metallophtalocyanines on other metal surfaces[4B, 4C].CO adsorption onto RuTPP is observed in the same image, but does not alter the adsorption site. It should be noted that other speicies such as dicarbonyl-RuTPP were not observed. The cross-sectional height profile demonstrates that CO-RuTPP has a larger apparent height than RuTPP, as shown in Fig. 1d, which is consistent with CO-MnPc/Bi(110)[4B], but different from CO-FePc/Au(111)[4A] and CO-CoTPP/Ag(111)[13], where CO adsorption reduces the apparent height of metalloporphyrins. This implies that the contribution of the CO to the STM image originates from a change in electronic structure rather than the height of the adsorbate. The electronic structure of RuTPP and CO-RuTPP on Cu(110) was studied using scanning tunnelling spectroscopy (STS). Fig. 2 shows STS spectra from the centre of RuTPP and CO-RuTPP after subtracting the reference signal from a bare Cu(110) surface. Due to the strongly nonlinear dependence of signal at high bias voltages, a reliable difference spectrum could only be obtained in the range of -1.3 to +0.9 V. RuTPP exhibits an increase in the *dI/dV* at a negative V_s. A distinct peak at around V_s=-1.1V was observed from both RuTPP (peak a') and CO-RuTPP (peak a). Such peaks derived from adsorbate-induced occupied states have been widely observed for metalloporphyrins on metal surfaces[14], e.g. the STS spectrum of CoTPP on Cu(110) reveals a peak at a negative sample bias of -0.72 eV, which was assigned to the highest occupied molecular orbital (HOMO) of CoTPP[14A]. We likewise assign our peak at V_s=-1.1 V to the RuTPP HOMO and note that it is not shifted by subsequent CO

adsorption. The most prominent peak introduced by the CO adsorption is the peak at around the Fermi level (peak c) but there also seems to be a more pronounced shoulder at V_s=-0.8 V (peak b)than for RuTPP/Cu(110).It should be noted that CO adsorption on CoTPP/Ag(111) did not produce any additional peaks in the range of -0.67 to +0.270 V[13].

In an attempt to link the observed peaks to adsorbate-induced electronic states, we have performed density functional calculations of the partial density of states of RuTPP/Cu(110) with and without adsorbed CO. The details of the calculational method and adsorption geometry are described in the supporting information. The results are shown in Fig. 2 and include partial density of states (PDOS) of partial waves of $d_\sigma(d_{z^2})$, $d_\pi(d_{xz}/d_{yz})$ and $d_\delta(d_{xy}/d_{x^2-y^2})$characters around the Ru atom, and p_z character around all C atom (Cπ). In the relevant energy range of around 1 eV below the Fermi level ε_F, RuTPP and CO-RuTPP possess states of all Rud characters and also of Cπ character, which could contribute to the LDOS probed by the STS. Upon CO adsorption, the changes in the PDOS relate to the formation of a π bond of the unoccupied CO 2π* with Rud_π (forming bonding and antibonding states) and a σ bond of the occupied CO 5σ with Rud_σ. As a result the d_σ and d_π states in the energy region below ε_F shift up and down in energy, respectively, whereas the downward shift of d_δ state in this region is not simply due to mixing with CO states. This latter state is not expected to contribute to the LDOS at the tip apex due to its high azimuthal angular momentum (m_l=2) as demonstrated by the calculated LDOS in the SI (Fig.S3).The behaviour of the double peak around -1 V in the STS upon CO adsorption is not easily reconciled by the behaviour of the corresponding peaks in the PDOS of d_π character. However, the CO-induced peak in the STS around ε_F can be reconciled with the calculated PDOS of d_σ and Cπ (and LDOS in Fig. S3). Note that the interpretation of STS in terms of electronic states is challenging, because in STS the electrons are either removed or added to the system, which in principle cannot be reproduced accurately by the calculated Kohn-Sham states.

We next studied the desorption of CO from CO-RuTPP/Cu(110) by tunnelling electrons from the STM tip to the centre of CO-RuTPP. After recording an STM image (Fig.3a), the tip was fixed over the centre of the CO-RuTPP and tunnelling electrons were injected into the molecule at a specific sample bias voltage with the feedback loop turned off. CO desorption appears as a sudden change in the tunnelling current in the I_t plot, as shown in Fig.3c. The desorption was confirmed by a subsequent STM image (Fig.3b), where a loss of CO is seen as a loss of the bright protrusion in the RuTPP centre. The desorption yield Y was calculated from Y = e/Iτ, where e is the elementary charge, and τ is the average time required for desorption. The desorbed CO can transfer to the vacuum, the tip or a neighbouring molecule[4B, 6]. The averaged values of Y(V_s) were obtained by repeating this experiment 10 times at each V_s. The desorption yield was recorded in the range of V_s=-1.075 to -1.60 V, as shown in Fig. 3d. No CO desorption was seen in the vibrational energy region below 400 mV at 4.7 K or77 K. Instead, we only observe an increase in the desorption probability at voltages below -1.1 V, followed by a plateau in the region of V_s=-1.15 to -1.45 V and an increase for above 1.45 V. The positive bias voltage above 0.9V does not show reproducible spectra. Below about -1.2 V, signal levels were sufficiently high to measure the current dependency of the desorption yield *Y* (Fig.3e). The slope of the double-log plot gives the exponent *n* in the power-law dependence[15]: $Y=I^n$, where n=2.1±0.2, 2.3±0.3, and 1.8±0.1 for V_s=1.25, 1.40, and 1.60 V, respectively. This power-law dependence on the applied current

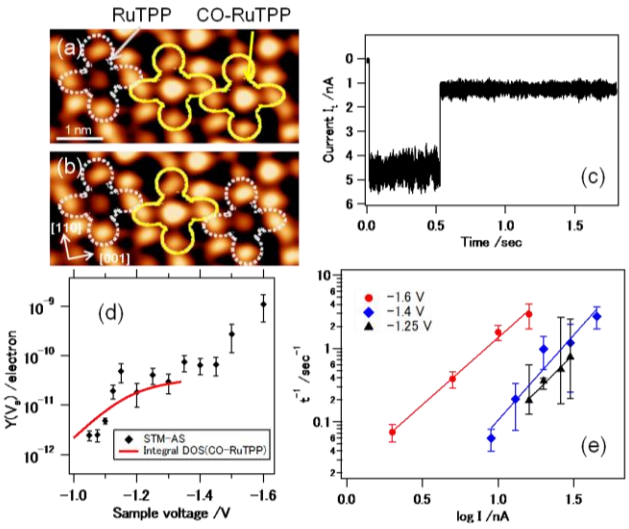

Fig.3 (a)–(b) STM images of CO-RuTPP adsorbed on Cu(110) (V_s= 500 mV, I_t = 0.5 nA)before and after injection of tunnelling electrons to the rightmost CO-RuTPP molecule as pointed by an arrow. RuTPP and CO-RuTPP are marked by dotted and solid lines, respectively. (c) Tunnelling current measured as a function of time under constant applied voltage (-1.5 V, 20 nA). (d) Reaction yield per electron for desorption of CO from CO-RuTPP/Cu(110) as a function of the sample bias voltage of the injected electrons. (e) CO desorption rate as a function of tunnelling current for V_s=-1.25, -1.40, and -1.60 V. The solid lines are the results of least squares fits to the data, whose slopes for the applied bias voltages correspond to powers (n) in the nonlinear power-law dependence. The error bars of (d) and (e) were determined from the standard deviation. The lower side of boundary of the error bar for -1.25 V in (e) is determined from the maximum desorption time.

shows that the desorption process consists of a two-carrier process, in the bias range of - 1.25 to-1.60V. This result is clearly different from NO desorption of NO-CoTPP/Au(111), which shows a change from a single electron process at V_s=0.8 V to a two electron process at V_s=1.0 V. The driving force for CO desorption can be explained by either the electric field effect or inelastic scattering of the tunnelling electrons. We can exclude an electric field effect, because it should result in a linear dependence of the desorption yield versus electric field in fixed I_t (sample bias per tip-sample distance)[16], unlike the dependence shown in Fig. 3d.

Next, we discuss the direct excitation of vibrational modes by IET as the origin of CO desorption. The desorption yield is too low at the sample voltage of below 1 V to enable measurements within a reasonable time scale. The desorption energy of CO from RuTPP/Cu(110) is ~0.75 eV which indicates that the C-O stretch mode is the only possible vibrational mode to realize desorption because the energies of the other modes are too low. Direct excitation of the C-O stretch mode is inefficient because of the lack of LDOS[17] at the vibrational energy range around 0.3 eV as shown in Fig.2.We can explain the increase in the desorption yield observed below -1 V and the subsequent plateau by the peak observed by STS around V_s=-1.1 V: while STS detects the LDOS at a specific V_s, the reaction yield in action spectroscopy reflects the integral over the same LDOS. An overlaid plot of the LDOS integral derived from STS (Fig 2) for CO-RuTPP shows the close correspondence between these two measurements in Fig.3d. A second threshold is observed at -1.5 V, which correlates with the calculated p states in Fig. 2, and was found to correspond again to a two electron process. We conclude that the IET process from the STM tip plays a dominant role in the desorption of CO between the V_s range of -1.075 and -1.5V.Since we are

operating at negative bias voltages, the underlying process must be a hole injection into occupied states, which then leads to desorption of CO. Desorption induced by hole injection and other chemical reactions have been previously reported in studies of adsorbates on metal substrates[8B, 18]. Applying a positive bias voltage does not show desorption of CO within a reasonable time scale, which can be assigned to a low LDOS of unoccupied states as seen in Fig.2. It should be noted that applying ahigh voltage (V_s>±1.5 V) can cause CO desorption non-locally which is assigned to the electric field effect as previously reported[4B, 8]. Fig.3(d) shows that CO desorption from RuTPP on Cu(110)has been already observed to begin at V_s=-1.075V. In contrast, CO desorption from a copper surface requires a bias voltage higher than 2.4V[6]. This difference cannot be explained by different desorption barriers, because the calculated CO adsorption energies on Ru-TPP/Cu(110) and Cu(110) are 1.5 and 1.1 eV (see, SI), respectively, as corroborated by the CO desorption temperature of CO-RuTPPbeing80 K higher than that of CO/Cu(110). The desorption mechanism of CO from a copper surface is electron injection to the unoccupied 2π* state, which occurs in a single-electron process[6]. A two-carrier process was not observed from CO on a copper surface, which was attributed to the short lifetime of the electronically excited state of around 0.8 to 5 fs[6]. As shown in Fig.3(e), we find that the lower desorption threshold voltage of CO-RuTPP/Cu(110) is due to the two-carrier process being much more effective than for Cu(110) but raises the question why it is more important for CO-RuTPP/Cu(110).Two-carrier induced IET process for single molecule reaction in such a wide V_s range is unique and so far has not been reported. At this stage, we are unable to conclude the details of desorption mechanism, but the observed threshold falls in the energy range of Rud states of CO-RuTPP/Cu(110) as discussed above. Here, we describe a probable scenario. Since our reaction thresholds are in the energy range of electronic excitations, we propose that the first hole excites CO-RuTPP to an electronically excited (positive ion) state. The second electron then leads to desorption by injecting a further hole. A single hole in the CO-RuTPP state at -0.8 V would be unlikely to result in desorption. This state is also present for Ru-TPP and is not influenced by the CO bonding while an efficient IET process would require the localization of the tunnelling electrons at the target chemical bond[19]. However, once a hole is injected in this state, lower occupied states might become energetically accessible to the second hole. For example, the states that originate from the hybridization between Rud_π and CO 2π* states[20], which contribute to the strength of the Ru-CO bond. Since these states are involved in the target chemical bond, their excitation could lead to relatively efficient desorption via vibrational excitation in analogy to desorption induced by electronic transition (DIET)[7] or simply withdrawing electrons from bonding states to induce repulsive CO-Ru potential. Such a process would be aided by an increase in the lifetimes of electronically excited states, which could originate from electronic decoupling of ruthenium from the copper substrate by CO adsorption, analogous to what has been observed for CO on phthalocyanines on metal substrates[4C]. The difference in desorption mechanism between CO from RuTPP and NO from CoTPP[8B], could lie in the degree of hybridization between CO/NO and TPP orbitals. NO is adsorbed in a tilted geometry, which means stronger hybridization between orbitals, which could make desorption possible over a wider energy range through carrier injection into any molecular orbitals.

In summary, CO desorption by inelastic tunnelling from CO-RuTPP on Cu(110) has been studied. STM imaging revealed that RuTPP and CO-RuTPP occupy a short bridge site, and CO adsorbs on atop of the ruthenium atom. Scanning tunnelling spectroscopy shows different HOMO levels of both RuTPP and CO-RuTPP in the same energy range where desorption by inelastic tunnelling sets in. The two-carrier process is probably caused by tunnelling of a second hole into an excited stated created by a hole tunnelling into a RuTPP or CO-RuTPP HOMO.

The authors thank to Dr.S.Haq, Dr.A.Massey, Dr.J.Oh and Dr.H-J.Yang for valuable discussions. T.O acknowledges IPA program at RIKEN and the University of Liverpool. P.P. and M.P. acknowledge computer time allocated on ARCHER through the Materials Chemistry Consortium (EPSRC grant no. EP/L000202)

Notes and references

1. J. P. Collman, J. I. Brauman, T. R. Halbert and K. S. Suslick, Proceedings of the National Academy of Sciences, 1976, 73, 3333-3337.
2. R. M. Ziff, E. Gulari and Y. Barshad, Physical Review Letters, 1986, 56, 2553-2556.
3. T. P. M. Goumans, A. W. Ehlers, M. C. van Hemert, A. Rosa, E.-J. Baerends and K. Lammertsma, Journal of the American Chemical Society, 2003, 125, 3558-3567.
4. (a)N. Tsukahara, E. Minamitani, Y. Kim, M. Kawai and N. Takagi, The Journal of chemical physics, 2014, 141, 054702; (b)A. Stróżecka, M. Soriano, J. I. Pascual and J. J. Palacios, Physical Review Letters, 2012, 109;147202(c) C. Isvoranu *et.al*, The Journal of Physical Chemistry C, 2011, 115, 24718-24727.
5. L. M. A. Levine and D. Holten, The Journal of Physical Chemistry, 1988, 92, 714-720.
6. L. Bartels, G. Meyer, K. H. Rieder, D. Velic, E. Knoesel, A. Hotzel, M. Wolf and G. Ertl, Physical Review Letters, 1998, 80, 2004-2007.
7. V. N. Ageev, Progress in Surface Science, 1994, 47, 55-203.
8. (a)S. R. Burema, K. Seufert, W. Auwärter, J. V. Barth and M.-L. Bocquet, ACS Nano, 2013, 7, 5273-5281; (b)H. Kim, Y. H. Chang, W.-J. Jang, E.-S. Lee, Y.-H. Kim and S.-J. Kahng, ACS Nano, 2015, 9, 7722-7728.
9. I. Horcas, R. Fernández, J. M. Gómez-Rodríguez, J. Colchero, J. Gómez-Herrero and A. M. Baro, Review of Scientific Instruments, 2007, 78, 013705.
10. (a)P. Donovan, A. Robin, M. S. Dyer, M. Persson and R. Raval, Chemistry – A European Journal, 2010, 16, 11641-11652; (b)W. Auwärter, D. Ecija, F. Klappenberger and J. V. Barth, Nat Chem, 2015, 7, 105-120.
11. B. G. Briner, M. Doering, H.-P. Rust and A. M. Bradshaw, Science, 1997, 278, 257-260.
12. S. Haq *et al*., Journal of the American Chemical Society, 2011, 133, 12031-12039.
13. K. Seufert, W. Auwärter and J. V. Barth, Journal of the American Chemical Society, 2010, 132, 18141-18146.
14. (a)V. C. Zoldan, R. Faccio, C. Gao and A. A. Pasa, The Journal of Physical Chemistry C, 2013, 117, 15984-15990;(b)T. G. Gopakumar, H. Tang, J. Morillo and R. Berndt, Journal of the American Chemical Society, 2012, 134, 11844-11847.
15. (a)B. C. Stipe *et al.* , Physical Review Letters, 1997, 78, 4410-4413; (b)D. M. Eigler, C. P. Lutz and W. E. Rudge, Nature, 1991, 352, 600-603.
16. M. Alemani, M. V. Peters, S. Hecht, K.-H. Rieder, F. Moresco and L. Grill, Journal of the American Chemical Society, 2006, 128, 14446-14447.
17. M. Ohara, Y. Kim, S. Yanagisawa, Y. Morikawa and M. Kawai, Physical Review Letters, 2008, 100, 136104.
18. (a)S. Alavi *et al.*, Physical Review Letters, 2000, 85, 5372-5375; (b)P. A. Sloan, M. F. G. Hedouin, R. E. Palmer and M. Persson, Physical Review Letters, 2003, 91, 118301.
19. Y. Sainoo, Y. Kim, T. Okawa, T. Komeda, H. Shigekawa and M. Kawai, Physical Review Letters, 2005, 95, 246102.
20. X. Y. Li and T. G. Spiro, Journal of the American Chemical Society, 1988, 110, 6024-6033.

